HTML ABSTRACT + LINKS

JOURNAL OF APPLIED PHYSICS **97**, 024510 (2005)

Organic magnetic-field-effect transistors and ultrasensitive magnetometers

Z. G. Yu,[a] M. A. Berding, and S. Krishnamurthy
SRI International, Menlo Park, California 94025

(Received 8 October 2004; accepted 14 October 2004; published online 27 December 2004)

We propose organic magetic-field-effect transistors and ultrasensitive magnetometers that exploit spin transport in organics and its sensitive dependence on a transverse magnetic field due to spin precession. The device design is based on experimentally observed magnetoresistance in magnet/polymer/magnet structures and on the theory of spin transport in these structures. It is shown that at room temperature the magnetometers are capable of detecting sub nT magnetic fields, and the I–V characteristics of the transistors can be strongly modified by magnetic fields of a few G with response times of a few ns. © *2005 American Institute of Physics*. [DOI: 10.1063/1.1831546]

Organic electronic devices such as organic light-emitting diodes and organic field-effect transistors have significant processing and performance advantages over their inorganic counterparts in low-cost and large-area applications.[1] Recently organics have been considered for spintronic devices,[2] for spins in organic materials are expected to last much longer than in inorganic materials because of the vanishing spin-orbit couplings. A major concern of using organics in spin devices, however, is their low carrier mobilities ($10^{-8}-1$ cm^2/V s), which adversely affect the device speed. In this article we show that *both* low mobilities and long spin lifetimes in organics can be exploited to make organic magetic-field-effect transistors (MFETs) and ultrasensitive magnetometers.

Our design is based on the theory on spin transport in magnet/polymer/magnet structures. In this theory, both magnetic-field-induced spin precession and electric-field-induced spin drift are consistently taken into account.[3] According to this theory, spin-dependent transport in organics can be strongly modified by magnetic-field-induced spin precession. Spin precession is very sensitive to the magnetic field in the polymer because the procession is controlled by the ratio, B/D, with B being the applied magnetic field and D the diffusion constant in the polymer (D and the mobility ν are related via $D=\nu k_B T/e$). Furthermore, extremely long spin relaxation times in polymers allow spin-polarized carriers to have ample time to precess without losing their spin coherence when they traverse the polymer. Another crucial ingredient in the device is that the half metallic magnets, such as $La_{0.7}Sr_{0.3}MnO_3$ (LSMO),[4] are used as contacts on which organics can be easily deposited, to ensure efficient spin injection into the polymer. Although spin precession has been exploited either electrically or optically in metals[5,6] and in semiconductors,[7–9] the proposed organic devices are novel because the functions of these devices rely on unique material properties in organics.

The device structure is illustrated in Fig. 1. It consists of an organic film on top of an insulator contacted by two LSMO electrodes. A metal strip beneath the insulator may be needed if an electrically controlled magnetic field is desired for a MFET. The basic device operation can be described as follows. Consider a device structure with the magnetizations of two LSMO contacts being antiparallel. In the absence of a transverse magnetic field, the device resistance is large because either spin species (up or down) must be the minority spin in one of the contacts and neither up-spin nor down-spin carriers can traverse the device easily. When a transverse magnetic field is applied, the spin orientation of carriers will vary over the distance in the polymer (spin precession), which provides a channel connecting the majority spins in the two LSMO contacts, and the resistance is therefore reduced. The electric field also strongly affects spin transport in the devices: (1) it considerably increases spin diffusion length through spin drift; (2) it determines the transit time of injected carriers in the device and modifies the resistance through the ratio of the transit time and the spin precession time (determined by the magnetic field). The feasibility of fabricating these spin devices is established by recent measurements of spin injections in LSMO/sexithienyl (T_6)/LSMO and LSMO/8-hydroxyquinolate aluminum (Alq_3)/Co structures even at room temperature.[10,11] T_6 and Alq_3 are two widely used materials in organic electronics. The observed I–V characteristics in LSMO/T_6/LSMO have been explained by our theory, indicating the validity of our theory.[3] In the proposed devices the magnetoresistance is achieved, not by changing the contact magnetizations, but by applying a transverse magnetic field (perpendicular to the contact magnetizations) to induce spin precession.

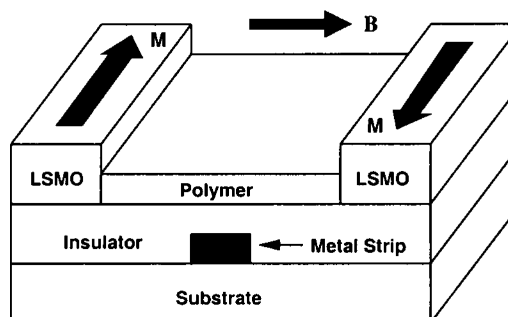

FIG. 1. Schematic device structure of organic MFET and magnetometer.

[a]Author to whom correspondence should be addressed; electronic mail: zhi-gang.yu.@sri.com

 © 2005 American Institute of Physics

Downloaded 22 Feb 2005 to 128.18.80.103. Redistribution subject to AIP license or copyright, see http://jap.aip.org/jap/copyright.jsp

A reliable prediction of the performance of these spin devices requires solving coupled spin-dependent transport equations with proper boundary conditions. The contact work functions and their relative position with respect to the electron- and hole-polaron levels in organics determine which type of carrier (electron or hole) is dominantly responsible for transport. We consider a single-carrier device in which the carriers are holes (electron devices can be analyzed similarly), which is appropriate for LSMO/T_6/LSMO and LSMO/Alq_3/Co structures. When a voltage is applied to a magnet/polymer/magnet structure, a spin-polarized current is injected into the polymer from the magnets, giving rise to spin accumulation in the polymer. To include spin precession in these magnetic structures, a 2×2 density matrix in spin space is needed, $\hat{\rho}^P=\rho_0^P\hat{\mathbf{1}}+\hat{\boldsymbol{\sigma}}.\boldsymbol{\rho}^P$, where $\rho_0^P\hat{1}$ is the equilibrium carrier distribution of the nonmagnetic polymer, and $\hat{\boldsymbol{\sigma}}=(\hat{\sigma}_x,\hat{\sigma}_y,\hat{\sigma}_z)$ are Pauli matrices. A general spin-dependent transport equation in the presence of electric field (current) and an external magnetic field reads[3]

$$\nabla^2\boldsymbol{\rho}^P-\frac{e\boldsymbol{E}}{k_BT}\cdot\nabla\boldsymbol{\rho}^P-\frac{\boldsymbol{\rho}^P}{L^2}-\boldsymbol{h}\times\boldsymbol{\rho}^P=0, \quad (1)$$

where $\boldsymbol{h}\equiv g\mu_B\boldsymbol{B}/\hbar D$ and $L=\sqrt{D\tau_S}$, with g being the gyromagnetic factor, μ_B the Bohr magneton, and τ_S spin lifetime. If the carriers are electrons, $\boldsymbol{E}$ in Eq. (1) should be replaced by $-\boldsymbol{E}$. The general solution to Eq. (1) has been obtained.[3] When the magnetic field is absent, the above equation describes the nonlinear spin transport due to the electric-field drift, which has been systematically studied in semiconductors.[12–14]

The magnets can be regarded as magnetic reservoirs in local equilibrium at chemical potentials $\mu^F_{\mathcal{L},\mathcal{R}}$, which is diagonal in spin space $\hat{\mu}^F_{\mathcal{L},\mathcal{R}}=\mu^F_{\mathcal{L},\mathcal{R}}\hat{1}$. Here $\mathcal{L}(\mathcal{R})$ denotes the left (right) magnet. The direction of the magnetization in each magnet is denoted by the unit vector $\boldsymbol{m}_{\mathcal{L},\mathcal{R}}$. For systems homogeneous in the lateral direction, the current leaving the left contact at $x=0$ is[15,16]

$$\hat{j}^C(0)=G^{\uparrow}\hat{u}^{\uparrow}_{\mathcal{L}}\left[\hat{\mu}^F_{\mathcal{L}}-\hat{\mu}^P(0)\right]\hat{u}^{\uparrow}_{\mathcal{L}}+G^{\downarrow}\hat{u}^{\downarrow}_{\mathcal{L}}\left[\hat{\mu}^F_{\mathcal{L}}-\hat{\mu}^P(0)\right]\hat{u}^{\downarrow}_{\mathcal{L}}$$
$$-G^{\uparrow\downarrow}\hat{u}^{\uparrow}_{\mathcal{L}}\hat{\mu}^P(0)\hat{u}^{\downarrow}_{\mathcal{L}}-G^{\downarrow\uparrow}\hat{u}^{\downarrow}_{\mathcal{L}}\hat{\mu}^P(0)\hat{u}^{\uparrow}_{\mathcal{L}}$$

and the current entering the right contact at $x=d$, $\hat{j}^C(d)$ can be similarly expressed.[3] Here $\hat{\mu}^P$ is the polymer electrochemical potential in the spin space. Operators $\hat{u}^{\uparrow(\downarrow)}_{\mathcal{L}}=1/2[1+(-)\hat{\sigma}.\boldsymbol{m}_{\mathcal{L}}]$ and $\hat{u}^{\uparrow(\downarrow)}_{\mathcal{R}}=1/2[1+(-)\hat{\sigma}.\boldsymbol{m}_{\mathcal{R}}]$ project spins to the magnetization directions of the magnets. $G^{\uparrow}(G^{\downarrow})$ is the electron conductance in the magnet with spin parallel (antiparallel) to the magnetization direction. $G^{\uparrow\downarrow}=\mathrm{Re}G^{\uparrow\downarrow}+i\mathrm{Im}G^{\uparrow\downarrow}$ is the mixing conductance, which measures the transport capability of spins oriented perpendicular to the magnetization direction. It is required that $\mathrm{Re}G^{\uparrow\downarrow}\geqslant(G^{\uparrow}+G^{\downarrow})/2$.[15,16]

The electrochemical potential $\hat{\mu}^P(=\mu_0^P\hat{1}+\hat{\boldsymbol{\sigma}}.\boldsymbol{\mu}^P)$ in the polymer is related to the density matrix $\hat{\rho}^P$. For nondegenerate systems with carriers following the Boltzmann distribution, we find

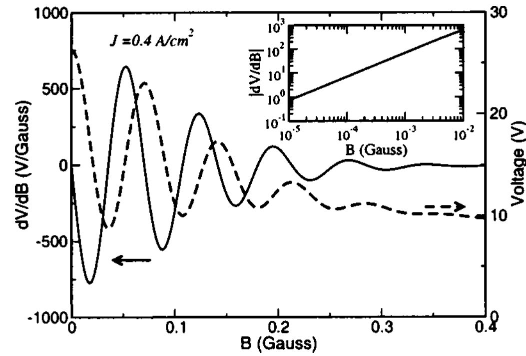

FIG. 2. Voltage (dashed line) and its differential response (solid line) as a function of transverse magnetic field with the constant current density $J=0.4\ \mathrm{A/cm^2}$ for an antiparallel structure. The inset plots the differential response for small magnetic fields in logarithmic scale.

$$\boldsymbol{\mu}^p=\frac{k_BT}{e}\frac{\rho^P}{2|\boldsymbol{\rho}^P|}\left[\ln\left(1+\frac{|\boldsymbol{\rho}^P|}{\rho_0^P}\right)-\ln\left(1-\frac{|\boldsymbol{\rho}^P|}{\rho_0^P}\right)\right] \quad (2)$$

and μ_0^P is determined by $d\mu_0^P/dx=-J/\sigma_p=-E$ with σ_p the conductivity of the polymer and $J=\mathrm{Tr}\hat{j}^P$ the total current. The requirement that the currents be continuous provides the following boundary conditions: (1) $\hat{j}^C(0)=\hat{j}^P(0)$ and (2) $\hat{j}^C(d)=\hat{j}^P(d)$, where the current in the polymer is computed via $\hat{j}^P(x)=\hat{\rho}^P(x)e\nu E-eDd\hat{\rho}^P/dx$. These two 2×2 matrix equations completely determine the solution to Eq. (1) for a given current J. The total resistance of the structure is then calculated via $R=(\mu^F_{\mathcal{L}}-\mu^F_{\mathrm{R}})/J$. We adopt in our calculations the parameters appropriate for the LSMO/T_6/LSMO structures, which have been obtained by fitting theoretical results to the experimental measurements.[3] $L=50$ nm, $\sigma_p=10^{-6}\ (\Omega\ \mathrm{cm})^{-1}$, $G^{\uparrow}=10^5\ \Omega\ \mathrm{cm}^2$, $G^{\downarrow}=10^{-2}\ \Omega\ \mathrm{cm}^2$, and $G^{\uparrow\downarrow}=0.7\times 10^5\ \Omega\ \mathrm{cm}^2$.

In Fig. 2 we plot the voltage drop V over a $d=200$ nm structure with antiparallel aligned LSMO contacts and its differential response, dV/dB, as a function of the transverse magnetic field with a constant current density, $J=0.4\ \mathrm{A/cm^2}$. The mobility is set to be $10^{-5}\ \mathrm{cm^2/V\ s}$. We see that as the magnetic field increases, the voltage across the device displays a damped oscillating behavior. The electric field in the device is $E=J/\sigma_p=4\times 10^5$ V/cm. Under this electric field, the spin transport distance (downstream spin diffusion length) at room temperature is

$$L_d=\left[-\frac{|eE|}{2k_BT}+\sqrt{\left(\frac{|eE|}{2k_BT}\right)^2+\frac{1}{L^2}}\right]^{-1}\simeq 4000\ \mathrm{nm}$$

which is longer than the device width. This electric-field drift effect on spin diffusion can be seen by setting $\boldsymbol{h}=0$ in Eq. (1). Similar effect also exists in nondegenerate semiconductors.[12–14] This explains why the magnetoresistance appears even though $L\ll d$. The oscilation in the magnetoresistance is attributed to the periodic spin precession angle within the carrier transit time τ_R ($\equiv d/\nu E$), $\theta_P=(\omega_L/2\pi)(d/\nu E)=dg\mu_BB/2\pi\nu E\hbar$.[3,8,9] The damping is due to the reduction of spin accumulation at the interfaces because of spin precession.[3] The differential response dV/dB measures the sensitivity of this device. We see that for some magnetic fields, dV/dB can be as high as 500 V/G. This

Downloaded 22 Feb 2005 to 128.18.80.103. Redistribution subject to AIP license or copyright, see http://jap.aip.org/jap/copyright.jsp

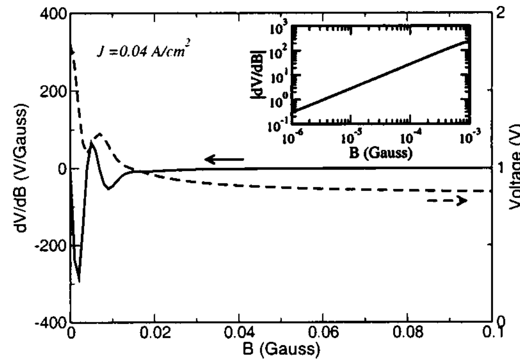

FIG. 3. Voltage (dashed line) and its differential response (solid line) as a function of transverse magnetic field with the constant current density $J=0.44\ \mathrm{A/cm^2}$. Other parameters are the same as in Fig. 2.

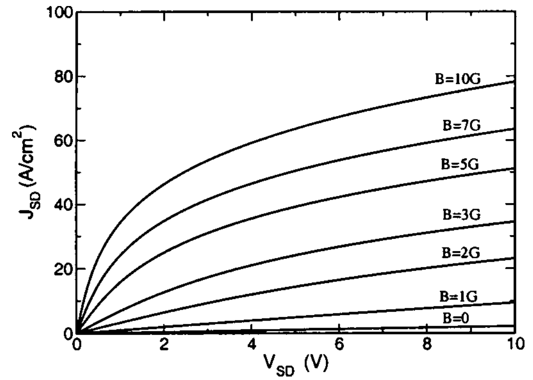

FIG. 4. Transistor current–voltage curves of an antiparallel structure exposed to different magnetic fields. $L=5000$ nm, $d=200$ nm, and $\nu=1\ \mathrm{cm^2/V\,s}$.

remarkable value indicates that a magnetic field change as small as $\Delta B=10^{-9}$ G (0.1 pT) will give rise to a readily measurable voltage change of 0.5 μV. Even at low magnetic fields around 10^{-5} G (1 nT), as shown in the inset of the figure, $dV/dB\simeq 1$ V/G, corresponding to $\Delta B=0.05$ nT for a voltage change of 0.5 μV. Thus this organic structure is an ultrasensitive magnetometer that can detect both small magnetic fields and small magnetic-field differences at sub nT levels. Figure 3 shows the voltage drop and its differential response in the same device structure as in Fig. 2, but with a smaller constant current density, $J=0.04\ \mathrm{A/cm^2}$. Again, we see that an ultrasensitive magnetometer is achieved under this current. In practice, the separation between the contacts, d, is not uniform throughout the device because of unavoidable contact roughness. However, since the ultrasensitive magnetometer is designed to detect extremely weak magnetic fields, i.e., within the first oscillating period (<0.05 G in Fig. 2), where the sensitivity dV/dB depends on the magnetic field almost linearly, the sensitivity will not be significantly compromised as long as the variation of d is relatively small.

The stong magnetic-field dependence of transport in these organic structures suggests that they can be used for organic MFETs, where the I–V characteristics are modified by a magnetic field. Since an efficient transistor requires a short response time, which is characterized by the transit time, τ_R, we use a very high mobility for organics, $\nu=1\ \mathrm{cm^2/V\,s}$ (as in pentacene), to describe MFETs. For such a high mobility, we estimate the spin diffusion length to be $L=5000$ nm (assume that the spin lifetime has a value of 10^{-6}–10^{-5} s and does not depend on the mobility) and the conductivity to be $\sigma_p=10^{-2}\ (\Omega\ \mathrm{cm})^{-1}$. In Fig. 4 we plot transistor current–voltage curves of an antiparallel structure exposed to different transverse magnetic fields using these parameters. We see the modification of the $I-V$ characteristics by different magnetic fields. These magnetic fields ($\leqslant 10$ G) are much weaker than the coercive field of the LSMO contacts (hundreds of G) and will not affect their magnetizations. Such transverse magnetic fields can also be created by supplying a current through the metal strip beneath the organic film, as shown in Fig. 1. The required current I can be estimated through $B=\mu_0 I/2\pi r$, where r is the distance between the polymer and the metal strip and μ_0 is the permeability. For $r=10$ nm, a current of 5 μA is needed to produce a magnetic field of 1 G. The typical response time (transit time) for such organic transistors is approximately $\tau_R\sim 4$ ns.

In summary, we have proposed organic MFETs and ultrasensitive magnetometers that exploit spin transport in organics and its sensitive dependence on a transverse magnetic field due to spin precession. These devices use quantum spin transport and therefore should be superior to other devices relying on classical charge/spin transport. The organic MFETs can be operated under magnetic fields as weak as a few G with response times of a few ns. The organic ultrasensitive magnetometers can detect both a small magnetic field and a small magnetic-field change at sub nT levels.

The authors thank Professor J. Shi for providing them with Ref. [11] prior to publication. This work was partly supported by IRAD from SRI International.

[1] See, e.g., I. H. Campbell and D. L. Smith, Solid State Phys. **55**, 1 (2001).
[2] See, e.g., S. A. Wolf, D. D. Awschalom, R. A. Buhrman, J. M. Daughton, S. von Molnár, M. L. Roukes, A. Y. Chtchelkanova, and D. M. Treger, Science **294**, 1488 (2001), and references therein.
[3] Z. G. Yu, M. A. Berding, and S. Krishnamurthy (unpublished).
[4] M. Cavallini, F. Biscarini, V. Dediu, P. Nozar, C. Taliani, and R. Zamboni, cond-mat/0301101.
[5] M. Johnson and R. H. Silsbee, Phys. Rev. Lett. **55**, 1790 (1985); Phys. Rev. B **37**, 5312 (1988).
[6] F. J. Jedema, H. B. Heersche, A. T. Filip, J. J. A. Baselmans, and B. J. van Wees, Nature (London) **416**, 713 (2002).
[7] J. Strand, B. D. Schultz, A. F. Isakovic, C. J. Palmstrom, and P. A. Crowell, Phys. Rev. Lett. **91**, 036602 (2003).
[8] A. M. Bratkovsky and V. V. Osipov, Phys. Rev. Lett. **92**, 098302 (2004).
[9] V. V. Osipov and A. M. Bratkovsky, Appl. Phys. Lett. **84**, 2118 (2004).
[10] V. Dediu, M. Murgia, F. C. Matacotta, C. Taliani, and S. Barbanera, Solid State Commun. **122**, 181 (2002).
[11] Z. H. Xiong, D. Wu, Z. V. Vardeny, and J. Shi, Nature (London) **427**, 821 (2004).
[12] A. G. Aronov and G. E. Pikus, Fiz. Tekh. Poluprovodn. (S.-Peterburg) **10**, 1177 (1976) [Sov. Phys. Semicond. **10**, 698 (1976)].
[13] Z. G. Yu and M. E. Flatté, Phys. Rev. B **66**, 201202 (R) (2002); **66**, 235302 (2002).
[14] I. Martin, Phys. Rev. B **67**, 014421 (2003).
[15] A. Brataas, Yu. V. Nazarov, and G. E. W. Bauer, Phys. Rev. Lett. **84**, 2481 (2000).
[16] D. H. Hernando, Yu. V. Nazarov, A. Brataas, and G. E. W. Bauer, Phys. Rev. B **62**, 5700 (2000).

Downloaded 22 Feb 2005 to 128.18.80.103. Redistribution subject to AIP license or copyright, see http://jap.aip.org/jap/copyright.jsp